

# Computation of Micro-stresses and interfacial Traction in Boron Carbide/AA7020 Alloy Metal Matrix Composites

<sup>1</sup>B. Kotiveera Chari and A. Chennakesava Reddy<sup>2</sup>

<sup>1</sup>Professor, Department of Mechanical Engineering, NIT, Warnagal, Andhra Pradesh, India

<sup>2</sup>Assistant Professor, Department of Mechanical Engineering, MJ College of Engineering and Technology, Hyderabad, India  
dr\_areddy@yahoo.com

**Abstract:** A micromechanical approach is developed to compute the micro stress within a metal matrix composite under various particle loading conditions. Square diamond unit cell/ellipsoid particle RVE models are analyzed and compared using two-dimensional finite element methods. Subsequently, effective material properties, the distribution of micro stress in the particle/matrix, as well as traction distribution at the particle–matrix interface, and the effect of different interfacial stiffness, are obtained.

**Keywords:** AA7020 alloy, boron carbide, RVE model, finite element analysis, interfacial tractions, ellipsoid particle.

## 1. INTRODUCTION

Metal matrix composites (MMCs) possess significantly improved properties including high specific strength; specific modulus, damping capacity and good wear resistance compared to unreinforced alloys. Following Taya and Chou [1] of using the combination of Eshelby's equivalent inclusion method and Mori-Tanaka's back stress analysis [2], Mochida et al. [3] obtained the weakened effective Young's modulus of particulate-reinforced DMMCs when some of particle reinforcements are damaged. The composite is modeled as an infinite elastic body which contains an infinite number of ellipsoidal inhomogeneities with two kinds (undamaged and damaged particles).

The objective of the present paper is to estimate micro stresses and interfacial tractions of boron carbide/AA7020 alloy metal matrix composites. Finite element analysis (FEA) of B<sub>4</sub>C/AA7020 alloy metal matrix composites was executed RVE models comprising of square diamond cell/ellipsoid particle.

## 2. MATERIALS AND METHODS

The matrix material was AA7020 alloy. The volume fractions of boron carbide particulate reinforcement were 10%, 20%, and 30%. The RVE scheme was selected to estimate micro stresses and interfacial tractions of metal matrix composites through finite element analysis as shown in figure 1. The shape of the particle was assumed to be elliptical in 2-dimensional form. The tensile loading was applied normal to the major axis of the elliptical particle. The perfect adhesion was assumed between boron carbide particle and AA7020 alloy matrix. PLANE183 element was employed for the matrix and the nanoparticle. The interface between particle and matrix was discretized using a COMBIN14 spring-damper element.

A linear stress–strain relation at the macro level can be formulated as follows:

$$\bar{\sigma} = \bar{C} \bar{\epsilon} \quad (1)$$

where  $\bar{\sigma}$  is macro stress, and  $\bar{\epsilon}$  represents macro total strain and  $\bar{C}$  and is macro stiffness matrix.

For plane strain conditions, the macro stress- macro strain relation is as follows:

$$\begin{Bmatrix} \bar{\sigma}_x \\ \bar{\sigma}_y \\ \bar{\tau}_{xy} \end{Bmatrix} = \begin{bmatrix} \bar{C}_{11} & \bar{C}_{12} & 0 \\ \bar{C}_{21} & \bar{C}_{22} & 0 \\ 0 & 0 & \bar{C}_{33} \end{bmatrix} \times \begin{Bmatrix} \bar{\epsilon}_x \\ \bar{\epsilon}_y \\ \bar{\gamma}_{xy} \end{Bmatrix} \quad (2)$$

The traction  $t$  at any point on the interface can always be decomposed into three components: normal traction  $t_n$ , which is perpendicular to the interface at the current point, tangential traction  $t_t$  which is tangent to the circumference of the particle at the current point, and longitudinal traction  $t_z$  which is parallel to the longitudinal direction of the particle. The interfacial tractions can be obtained by transforming the micro stresses at the interface as given in Eq. (3):

$$t = \begin{Bmatrix} t_z \\ t_n \\ t_t \end{Bmatrix} = T\sigma \quad (3)$$

where,  $T = \begin{bmatrix} 0 & 0 & 0 \\ \cos^2\theta & \sin^2\theta & 2\sin\theta\cos\theta \\ -\sin\theta\cos\theta & \sin\theta\cos\theta & \cos^2\theta - \sin^2\theta \end{bmatrix}$

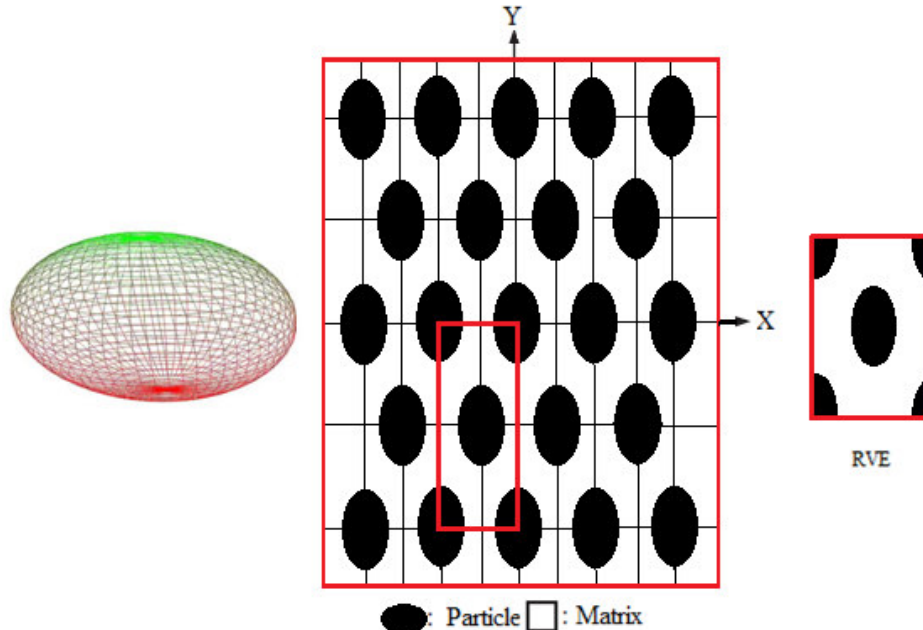


Figure 1: The RVE model: (a) particle distribution in square diamond array and (b) RVE scheme.

### 3. RESULTS AND DISCUSSION

The effective material properties of B<sub>4</sub>C/AA7020 alloy metal matrix composites are showed in figure 2. The elastic moduli, E<sub>x</sub> and E<sub>y</sub> increase with increase of volume fraction of boron carbide (figure 2a). The shear modulus decreases with increase of volume fraction of boron carbide in the composite (figure 2c). Elastic modulus of boron carbide particle in the longitudinal direction is higher than that of the matrix, particle dominates the longitudinal stiffness (E<sub>x</sub> > E<sub>m</sub>) of the composite. On the other hand, since Poisson's ratio of the composite is unaffected by the addition of the boron carbide particle to the matrix AA 7020 alloy (figure 2b).

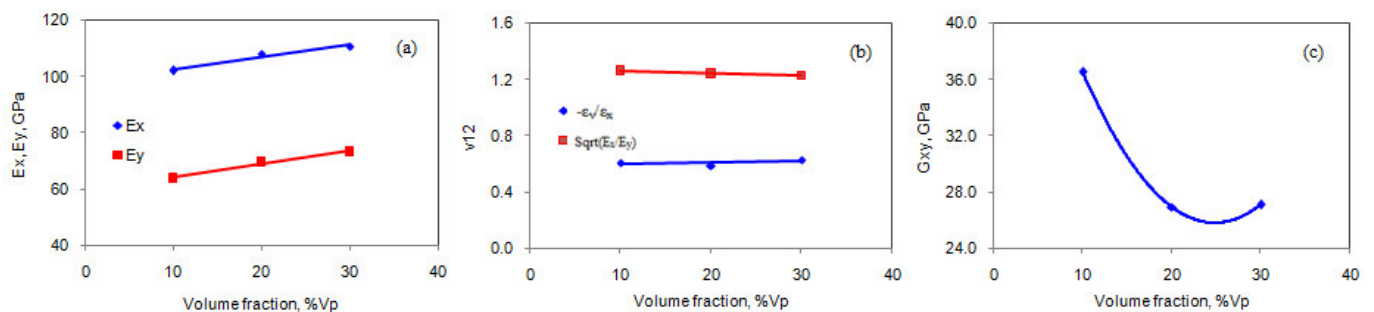
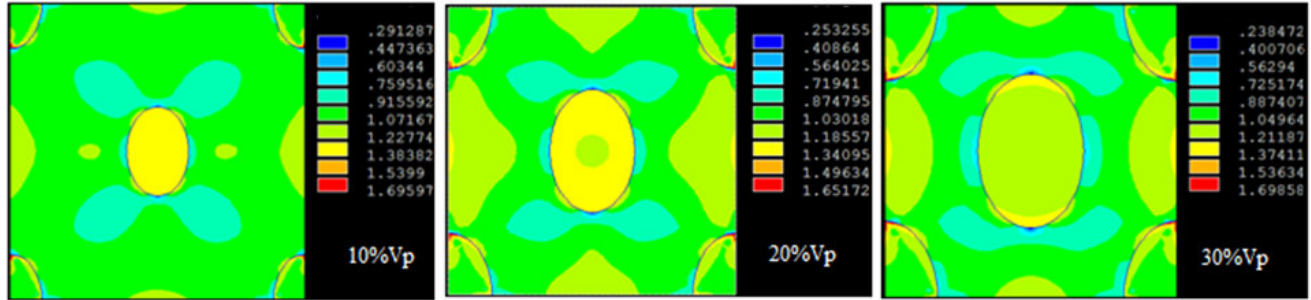
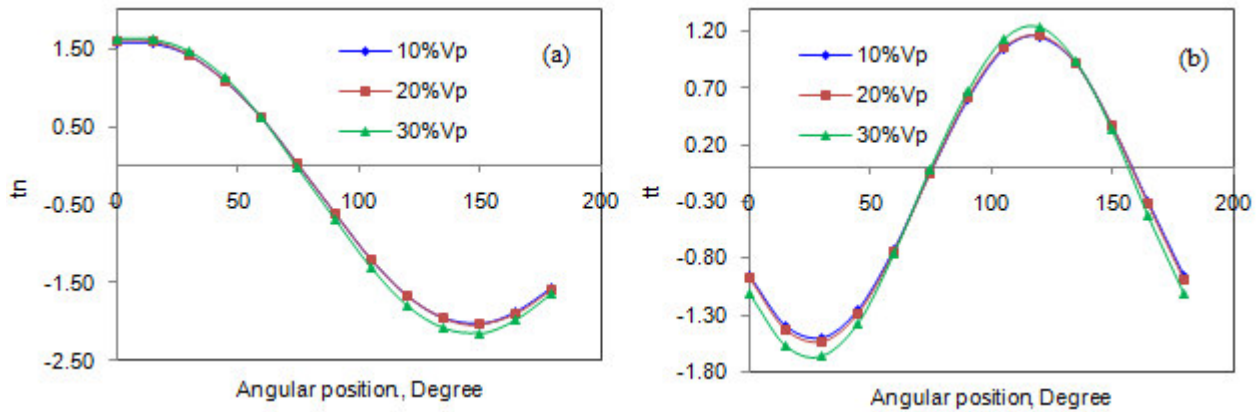


Figure 2: Effect of volume fraction on effective material properties.



**Figure 3:** von Mises stress induced in  $B_4C/AA7020$  alloy metal matrix composites.

Figure 3 shows stress concentrations developed in a unit cell of square diamond array under tensile stress. In a unit cell of square diamond array under tensile stress, maximum stress (yellow, green and red colors) concentrations are observed in the particle or at the neighboring region of the particle–matrix interface. The regions of minimum stress (light blue color) concentrations align with transverse direction of tensile loading at the particle–matrix interface. The direction of macro load coincides with the direction of  $t_n$  at  $\theta = 0^\circ$ , so  $t_n$  attains its maximum; as  $\theta$  increases unto  $150^\circ$ , the component of the macro load in the normal direction of the interface decreases, so  $t_n$  also decreases (figure 4a). Poisson’s effect causes compression, so  $t_n$  reaches the minimum (might be negative) at  $150^\circ$ . The tangential traction  $t_t$  decreases as  $\theta$  increases from  $0^\circ$ , and reaches the minimum at  $30^\circ$  and then increases until  $\theta = 120^\circ$  (figure 4b).



**Figure 4:** Interfacial tractions along the angle due to tensile loading: (a) normal and (b) tangential.

#### 4. CONCLUSION

For effective material properties, variations of  $E_x$ ,  $E_y$ ,  $G_{xy}$  and  $\nu_{12}$  with respect to  $V_p$ , are predicted. For boron carbide/AA7020 alloy metal matrix composites, the interfacial normal traction decreases from  $0^\circ$  to  $150^\circ$ . The interfacial tangential traction increases from  $30^\circ$  to  $120^\circ$ .

#### REFERENCES

1. M. Taya and T.-W. Chou, On two kinds of ellipsoidal inhomogeneities in an infinite elastic body: an application to a hybrid composite, *Int. J. Solids Structures*, vol. 17, pp. 553-563, 1981.
2. T. Mori and K. Tanaka, Average stress in matrix and average elastic energy of materials, *Acta Meta/1.*, vol. 21, pp. 571-574, 1973.
3. T. Mochida, M. Taya and M. Obata, Effect of damaged particles on the stiffness of a particle/metal matrix composite, *JSME Int. J., Series I*, vol. 34, pp. 187-193, 1991.